Article

Novel Oxysterols Have Pro-Osteogenic and Anti-Adipogenic Effects In Vitro and Induce Spinal Fusion In Vivo

Jared S. Johnson[1#], Vicente Meliton[2#], Woo Kyun Kim[2], Kwang-Bok Lee[1], Jeffrey C. Wang[1], KhanhLinh Nguyen[3], Dongwon Yoo[3], Michael E. Jung[3], Elisa Atti[4], Sotirios Tetradis[4], Renata C. Pereira[5], Clara Magyar[6], Taya Nargizyan[2], Theodore J. Hahn[7], Francine Farouz[8], Scott Thies[8], Farhad Parhami[2]*

[1]Department of Orthopedic Surgery, UCLA, Los Angeles, California, USA
[2]Department of Medicine, David Geffen School of Medicine, UCLA, Los Angeles, California, USA
[3]Department of Chemistry and Biochemistry, UCLA, Los Angeles, California, USA
[4]School of Dentistry, UCLA, Los Angeles, California, USA
[5]Department of Pediatric Nephrology, UCLA, Los Angeles, California, USA
6Department of Pathology and Laboratory Medicine, UCLA, Los Angeles, California, USA
[7]VA Greater Los Angeles Healthcare System and Geriatric Research, Education, and Clinical Center, Los Angeles, California, USA
[8]Fate Therapeutics, Inc., San Diego, California, USA

[#] These authors have contributed equally to this manuscript.

[*] **Corresponding Author:**
Farhad Parhami, Ph.D.
David Geffen School of Medicine at UCLA
Center for the Health Sciences, A2-237
10833 Le Conte Avenue
Los Angeles, California, 90095
Tel: 310-825-5729
Fax: 310-206-9133
Email: fparhami@mednet.ucla.edu

Received 19 January 2011; Accepted 18 February 2011
Journal of Cellular Biochemistry

DOI 10.1002/jcb.23082

Abstract

Stimulation of bone formation by osteoinductive materials is of great clinical importance in spinal fusion surgery, repair of bone fractures, and in the treatment of osteoporosis. We previously reported that specific naturally occurring oxysterols including 20(*S*)-hydroxycholesterol (20S) induce the osteogenic differentiation of pluripotent mesenchymal cells, while inhibiting their adipogenic differentiation. Here we report the characterization of two structural analogs of 20S, Oxy34 and Oxy49, which induce the osteogenic and inhibit the adipogenic differentiation of bone marrow stromal cells (MSC) through activation of Hedgehog (Hh) signaling. Treatment of M2-10B4 MSC with Oxy34 or Oxy49 induced the expression of osteogenic differentiation markers Runx2, Osterix (Osx), alkaline phosphatase (ALP), bone sialoprotein (BSP) and osteocalcin (OCN), as well as ALP enzymatic activity and robust mineralization. Treatment with oxysterols together with PPARγ activator, troglitazone (Tro), inhibited mRNA expression for adipogenic genes PPARγ, LPL, and aP2, and inhibited the formation of adipocytes. Efficacy of Oxy34 and Oxy49 in stimulating bone formation in vivo was assessed using the posterolateral intertransverse process rat spinal fusion model. Rats receiving collagen implants with Oxy 34 or Oxy49 showed comparable osteogenic efficacy to BMP2/collagen implants as measured by radiography, MicroCT, and manual inspection. Histological analysis showed trabecular and cortical bone formation by oxysterols and rhBMP2 within the fusion mass, with robust adipogenesis in BMP2-induced bone and significantly less adipocytes in oxysterol-induced bone. These data suggest that Oxy34 and Oxy49 are effective novel osteoinductive molecules and may be suitable candidates for further development and use in orthopaedic indications requiring local bone formation.

Key Words: Oxysterols, Spinal Fusion, BMP2, Osteogenesis, Adipogenesis

Introduction

Repair of skeletal disorders through localized induction of bone formation is of major clinical significance in orthopedic procedures such as spinal fusion and repair of segmental defects and bone fractures [Mundy, 2002; Rodan and Martin, 2002; Johnson and Urist, 2000; Yoon and Boden, 2002] . Posterolateral lumbar spinal fusion, in which new bone formation is induced between two or more vertebrae, is a common surgical procedure used to manage back pain associated with disc degeneration, herniated disc, and other lower back disorders when conservative measures have failed or are inappropriate [Lipson, 2004; Cahill et al, 2009; Hsu and Wang, 2008]. The current gold standard for stimulating bone formation in spinal fusion is autogenous bone graft [Franceschi, 2005]. About 1.5 million bone-grafting surgeries are performed in the United States annually [Brown et al, 2006]. The use of autogenous bone grafting is especially attractive since it increases the rate of fusion and since non-fusion or incomplete fusion can result in significant pain and a possible need for reoperation. Although the use of autogenous bone grafting is successful in increasing the rate of fusion, it is also associated with significant donor-site morbidity, increased operative times, and blood loss [Rihn et al, 2010; Vaccaro et al, 2002; Arrington et al, 1996]. In addition to causing potential complications, the use of autogenous bone grafting is not a suitable option for all patients, including those undergoing extensive multilevel surgery in which the amount of bone collected from a donor site is insufficient. Similarly, the use of autogenous bone graft may not be effective in patients with medical conditions that affect bone quality such as osteoporosis, Paget's disease, diabetes, and cancer. The prevalence of surgeries in which bone grafts are used, and the limitations of using autogenous bone grafts, have led to a significant interest in developing suitable substitutes that

induce bone formation when applied locally to areas of bone defect [Franceschi, 2005; Vaccaro et al, 2002; Miyazaki et al, 2009; Habibovic and de Groot, 2007].

Bone morphogenic proteins (BMPs), members of the transforming growth factor-beta (TGF-β) superfamily, have received particular attention due to their potent osteoinductive properties [Axelrod and Einhorn, 2009; Bessa et al, 2008; Zhu et al, 2004]. Currently, recombinant human BMP2 (rhBMP2) and rhBMP7, are approved for orthopaedic clinical use in the United States [Khosla et al, 2008; Gautschi et al, 2007]. Although these proteins have been proven in clinical trials to significantly increase fusion rates comparable to autogenous bone graft, their use can be limited by high cost and potential adverse effects [Cahill et al, 2009; Hsu and Wang, 2008; Axelrod and Einhorn, 2009; Glassman et al, 2010]. Recent reports have demonstrated rhBMP2-induced inflammatory reactions that are especially problematic in procedures involving the cervical spine, with the risk of airway compromise and ectopic bone formation [Hsu and Wang, 2008; Axelrod and Einhorn, 2009; Chen et al, 2010; Garrett et al, 2010; Shahlaie and Kim, 2008]. In addition, concerns about BMPs' increasing potential risks of carcinogenicity and teratogenicity have also been noted [Bieniasz et al, 2009; Langenfeld et al, 2003; Gordon et al, 2009]. These limitations have prompted the further investigation for safe and cost-effective osteoinductive compounds to stimulate localized bone formation in orthopaedic procedures.

We previously reported that specific naturally occurring oxysterols have potent osteoinductive and anti-adipogenic properties when administered to various multipotent mesenchymal cells and osteoprogenitors in vitro, and that they modestly induce bone formation in a rat calvarial defect model in vivo [Kha et al, 2004; Richardson et al, 2007; Amantea et al, 2008; Dwyer et al, 2007; Kim et al, 2007; Aghaloo et al, 2007]. Furthermore, we reported that

the osteoinductive and anti-adipogenic effects of these oxysterols are mediated through activation of the Hedgehog (Hh) signaling pathway [Dwyer et al, 2007; Kim et al, 2007; Kim et al, 2010]. Given that Hh signaling plays an important role in skeletal development and the maintenance and repair of bone in adult organisms [Varjosalo and Taipale, 2008; Lum and Beachy, 2004; Simpson et al, 2009; Ito H et al, 1999], we suggested that oxysterols that activate Hh signaling in osteoprogenitor cells may offer a novel strategy for localized and/or systemic therapeutic stimulation of new bone formation [Khat et al, 2004; Richardson et al, 2007; Kim et al, 2007]. Although the reported naturally occurring oxysterols had osteoinductive effects in vitro when used at micromolar doses, they had only modest effects in inducing new bone formation in vivo [Aghaloo et al, 2007]. Therefore, we aimed at designing new analogs of the most potent naturally occurring osteoinductive oxysterol, 20(*S*)-hydroxycholesterol (20S), with improved in vitro and in vivo osteoinductive activity. In this article we report on the synthesis and characterization of two potent structural analogs of 20S, Oxy34 and Oxy49. These molecules robustly induce the osteogenic differentiation of bone marrow stromal cells (MSC) and inhibit their adipogenic differentiation in vitro through activation of Hh signaling. In addition, they effectively stimulate new bone formation and spinal fusion in vivo when administered locally in a previously reported clinically relevant rat posterolateral spinal fusion model [Miyazake and Morishita et al, 2008; Miyazake and Sugiyama et al, 2008; Alanay et al, 2008]. The bone forming effects of oxysterols in vivo are comparable to that of rhBMP2, but are not associated with the robust adipogenesis observed with rhBMP2.

Materials and Methods

Cell culture and reagents

Mouse multipotent bone marrow stromal cell (MSC) line, M2-10B4 (M2), and embryonic fibroblast cells line C3H10T1/2 were purchased from American Type Culture Collection (Rockville, MD, USA) and maintained as we have previously described [Kha et al, 2004; Richardson et al, 2007; Dwyer et al, 2007; Kim et al, 2007; Kim et al, 2010]. Treatments to induce osteogenic differentiation were performed in RPMI 1640 medium (Irvine Scientific, Santa Ana, CA, USA) containing 5% heat-inactivated fetal bovine serum (FBS, Hyclone, Logan, UT, USA), 50 μg/ml ascorbate, and 3 mM β-glycerophosphate (BGP). Adipogenic treatments were performed under similar conditions but without the addition of ascorbate and BGP. Cyclopamine (Cyc) was purchased from EMD Biosciences, Inc (La Jolla, CA, USA) and troglitazone (Tro) from BioMol Research Laboratories (Plymouth Meeting, PA, USA). For in vivo studies, sterile absorbable collagen sponges (Helistat, Integra Life Sciences, Plainsboro, NJ, USA) were cut into pieces measuring 5x5x15 mm. Dilutions of oxysterols were prepared in 100% dimethyl sulfoxide (DMSO) and just prior to implantation, the prepared collagen sponges were soaked in 50 μl of Oxy34 or Oxy49, while control sponges were soaked in 50 μl of DMSO.

Quantitative RT-PCR

Total RNA was extracted using Trizol from Invitrogen (Carlsbad, CA, USA) according to the manufacturer's instructions and single stranded cDNA prepared as we have previously described [Dwyer et al, 2007; Kim et al, 2010]. Q-RT-PCR reactions were performed using iQ SYBR Green Supermix and an iCycler RT-PCR Detection System (Bio-Rad, Hercules, CA, USA). Primer sequences used were previously reported [Dwyer et al, 2007; Kim et al, 2007; Kim et al, 2010].

Alkaline phosphatase activity assay and Oil red O staining

Colorimetric alkaline phosphatase (ALP) activity assay on whole cell extracts was performed as we have previously described [Kha et al, 2004]. Oil red O staining for detection of adipocytes was performed as previously described [Kim et al, 2007], and the number of adipocytes was quantified by counting Oil red O-positive cells in five separate fields per well, in three wells per experimental condition.

Transient transfection and Gli-dependent reporter assay

Cells at 70% confluence in 24-well plates were transiently transfected with Gli-dependent firefly luciferase and Renilla luciferase vectors as we have previously described [Dwyer et al, 2007; Kim et al, 2010]. Total DNA per well did not exceed 500 ng, and FuGENE 6 transfection reagent (Roche Applied Science, Indianapolis, IN, USA) was used at a ratio of 3:1. Cells were treated for 48 hours before luciferase activity was assessed using the Dual Luciferase Reporter Assay System (Promega Corporation, Madison, WI, USA) according to manufacturer's instructions.

^{45}Ca incorporation assay

Matrix mineralization in cell monolayers was quantified using the ^{45}Ca incorporation assay as previously described [Kha et al, 2004].

Synthesis and molecular characterization of oxysterols

Materials were obtained from commercial suppliers and were used without further purification. Air or moisture sensitive reactions were conducted under argon atmosphere using oven-dried glassware and standard syringe/septa techniques. The reactions were monitored on silica gel TLC plates under UV light (254 nm) followed by visualization with a *p*-anisaldehyde or ninhydrin staining solution. Column chromatography was performed on silica gel 60. ^{1}H NMR

spectra were measured at 400 MHz in $CDCl_3$ unless stated otherwise and data were reported as follows in ppm (d) from the internal standard (TMS, 0.0 ppm): chemical shift (multiplicity, integration, coupling constant in Hz.). The following is a stepwise description of the protocols used to synthesize Oxy34 and Oxy49:

3β-(1,1-Dimethylethyl)dimethylsilyloxy))cholest-3-en-20*S*-ol, 2. To a stirred solution of 20*S*-hydroxycholesterol **1** (18.0 mg, 0.045 mmol) and imidazole (9.1 mg, 0.134 mmol) in DMF (3 mL) was added TBSCl (8.8 mg, 0.058 mmol) at 0 °C. The reaction was allowed to warm to 23 °C and stirred overnight. The reaction was quenched with 50% NH_4Cl (10 mL) and extracted with diethyl ether (15 mL). The combined organic layers were dried over $MgSO_4$, concentrated under vacuum and purified by column chromatography (33% ethyl acetate in hexane) to yield 21.3 mg (92%) of **2** as a white solid. ^{1}H NMR δ 5.31 (m, 1H), 3.48 (m, 1H), 2.31-0.83 (m, 27H), 1.27 (s, 3H), 1.00 (s, 3H), 0.89 (s, 9H), 0.87 (d, 6H, J = 6.7 Hz), 0.86 (s, 3H), 0.05 (s, 6H).

3β-(1,1-Dimethylethyl)dimethylsilyloxy)cholestane-6α,20*S*-diol, 3. To a solution of alcohol **2** (1.4 g, 2.71 mmol) in anhydrous THF (60 mL) at 0 °C was added 1.0 M of borane in THF (15 mL, 15 mmol). The reaction was allowed to warm to 20 °C over 5 h. A mixture of 10% NaOH (56 mL) and 33% H_2O_2 (75 mL) was added at 0 °C and warmed to 20 °C over 4 h. The reaction mixture was extracted three times with diethyl ether (30 mL x 3). The organic phases were collected, dried over $NaSO_4$ and evaporated *in vacuo* to afford an oil as a 10:1 mixture of diastereomers. Purification by flash column chromatography (silica gel, 1:1 hexane/diethyl ether v/v) afforded the diol **3** (1.0 g, 69%) as a white solid. ^{1}H NMR δ 3.50 (1H, dddd, J = 11.2, 11.2, 4.4, 4.4 Hz), 3.40 (1H, ddd, J = 10.8, 10.8, 4.4 Hz), 2.03 – 1.31 (21H, m), 1.23 – 1.0 (9H, m), 0.87 (9H, s), 0.85 (3H, s), 0.81 (6H, d, J = 8.0 Hz), 0.80 (3H, s), 0.04 (6H, s). ^{13}C NMR ($CDCl_3$, 100 MHz) δ: 75.2, 72.0, 69.5, 57.6, 56.3, 53.8, 51.8, 44.2, 42.9, 41.4, 40.2, 39.6, 37.4, 36.3,

33.6, 32.6, 31.6, 27.9, 26.4, 25.9, 23.7, 22.7, 22.6, 22.3, 22.1, 21.0, 18.2, 13.9, 13.5, -4.5. FTIR ($CHCl_3$): 3411, 2949, 1245, 1082 cm^{-1}.

Oxy34. (3*S*,6*S*,8*R*,9*S*,10*R*,13*S*,14*S*,17*S*)-17-((*S*)-2-Hydroxy-6-methylheptan-2-yl)-10,13-dimethylhexadecahydro-1*H*-cyclopenta[*a*]phenanthrene-3,6-diol (Cholestan-3β,6α,20*S*-triol). To a solution of the silyloxydiol **3** in THF (3.0 mL) was added a 1.0 M solution of tetrabutylammonium fluoride in THF (1.0 mL, 1.0 mmol). After stirring for 12 h at 20 °C, the reaction was treated with water and extracted three times with diethyl ether and the organic layer was washed with saturated NaCl. The organic phases were collected, dried over Na_2SO_4 and concentrated *in vacuo* to give an oil. Flash column chromatography of this oil (silica gel, 1:4 hexane/diethyl ether) yielded the desired triol **Oxy34** (64 mg, 80%) as a white powder. ^{1}H NMR δ 3.61 – 3.53 (1H, dddd, *J* = 11.0, 11.0, 4.8, 4.8 Hz), 3.41 (1H, ddd, *J* = 10.7, 10.7, 4.4 Hz), 2.17 – 1.40 (18H, m), 1.25 (3H, s), 1.23 – 1.0 (13H, m), 0.86 (6H, d, *J* = 6.6 Hz), 0.83 (3H, s), 0.81 (3H, s). ^{13}C NMR ($CDCl_3$, 100 MHz) δ: 75.2, 71.2, 69.5, 57.7, 56.3, 53.7, 51.7, 44.2, 42.9, 41.5, 40.2, 39.6, 37.3, 36.3, 33.6, 32.2, 31.0, 27.9, 26.4, 23.7, 22.7, 22.6, 22.3, 22.0, 21.0, 13.8, 13.5. FTIR ($CHCl_3$): 3363, 2929 cm^{-1}. Melting point: 172-174 °C.

(3*S*,8*S*,9*S*,10*R*,13*S*,14*S*,17*S*)-10,13-Dimethyl-17-(2-methyl-1,3-dioxolan-2-yl)-2,3,4,7,8,9,10,11,12,13,14,15,16,17-tetradecahydro-1*H*-cyclopenta[*a*]phenanthren-3-yl acetate, 4. To a solution of pregnenolone acetate (11.4 g, 32 mmol) in 160 mL benzene were added pyridinium *p*-toluenesulfonate (1.61 g, 6.4 mmol) and ethylene glycol (5.5 mL, 6.12 g, 98.6 mmol). The mixture was refluxed under a Dean-Stark apparatus at 110 °C for 12 h. The reaction mixture was diluted with diethyl ether, washed sequentially with water and satd. NaCl, dried over Na_2SO_4 and concentrated *in vacuo.* Purification of the crude solid by recrystallization from hot hexane provided the ketal **4** (10 g, 78%) as colorless crystals. ^{1}H NMR ($CDCl_3$, 400

MHz) δ: 5.37 – 5.36 (1H, m), 4.59 (1H, dddd, J = 12.6, 12.6, 4.4, 4.4 Hz), 4.02 – 3.82 (4H, m), 2.32 – 2.29 (1H, m), 2.02 (3H, s), 1.87 – 1.43 (16H, m), 1.29 (3H, s), 1.23 – 1.06 (3H, m), 1.01 (3H, s), 0.77 (3H, s).^{13}C NMR ($CDCl_3$, 100 MHz) δ: 170.5, 139.7, 122.5, 112.0, 74.0, 65.2, 63.2, 58.2, 56.5, 50.0, 41.8, 39.4, 38.1, 37.0, 36.6, 31.8, 31.4, 27.8, 24.6, 23.8, 23.0, 21.4, 20.8, 19.3, 12.9. FTIR ($CHCl_3$): 2940, 1730, 1359, 1255, 1032 cm^{-1}. Melting point: 110-112 °C.

1-((3*S*,5*S*,6*S*,8*R*,9*S*,10*R*,13*S*,14*S*,17*S*)-3,6-Bis-[(1,1-dimethylethyl)dimethylsilyloxy]-10,13-dimethylhexadecahydro-1*H*-cyclopenta[*a*]phenanthren-17-yl)ethanone, 5. To a solution of the ketal **4** (5.0 g, 12 mmol) in THF (150 mL) cooled to 0 °C was added 1.0 M of borane in THF (40.0 mL, 40 mmol). The reaction was allowed to warm to 20 °C over 5 h. A mixture of 150 mL of NaOH (10%) and 75 mL of H_2O_2 (33%) was then added at 0 °C and the mixture was allowed to warm to 20 °C over 4 h. The reaction mixture was extracted with diethyl ether (3 x 100 mL). The organic phases were collected, dried over Na_2SO_4 and evaporated *in vacuo* to afford an oil. The crude acetal diols (5.1 g, 13.5 mmol) were dissolved in acetone (250 mL) and treated with 1M HCl (50 mL, 50 mmol). After 30 min under reflux, the resulting mixture was quenched with 1M NaOH at 0 °C and the organic solvent was evaporated. The aqueous layer was extracted with diethyl ether (3 x 50 mL). The organic layer was washed with saturated NaCl, dried over Na_2SO_4 and concentrated under reduced pressure. The crude ketone (4.32 g, 12.9 mmol) was dissolved in anhydrous dimethylformamide (DMF, 50 mL) and imidazole (15.0 g. 22 mmol) was added. The reaction was allowed to stir for 20 min followed by slow addition of *tert*-butyldimethylsilyl chloride (9.8 g, 65 mmol). After stirring for 12 h at ambient temperature, the reaction mixture was quenched with water and extracted three times with diethyl ether (150 mL x 3). The organic layers were washed with 1 M NaOH, dried over Na_2SO_4, and evaporated *in vacuo* to give an oil. Purification of this crude residue by column

chromatography (silica gel, 5:1 hexane/diethyl ether v/v) afforded the bis(*tert*-butyldimethylsilyloxy) ketone **5** (3.5 g, 52% over three steps) as a white powder. ^{1}H NMR ($CDCl_3$, 400 MHz) δ: 3.47 (1H, dddd, J = 11.0, 11.0, 4.8, 4.8 Hz), 3.36 (1H, ddd, J = 10.4, 10.4, 4.4 Hz), 2.53 (1H, d, J = 8.8, 8.8 Hz), 2.20 – 2.14 (1H, m), 2.10 (3H, s), 2.01 – 1.97 (1H, m), 1.88 – 1.82 (1H, m), 1.73 – 0.89 (17H, m), 0.88 (18H, s), 0.79 (3H, s), 0.59 (3H, s), 0.043 (3H, s), 0.040 (3H, s), 0.03 (3H, s), 0.02 (3H, s). ^{13}C NMR ($CDCl_3$, 100 MHz) δ: 209.5, 72.2, 70.1, 63.7, 56.4, 53.7, 51.8, 44.2, 41.9, 38.9, 37.6, 36.3, 34.3, 33.2, 31.7, 31.5, 25.94, 25.92, 24.4, 22.7, 21.1, 18.3, 18.1, 13.5, 13.4, -4.06, -4.61, -4.69, -4.73. FTIR ($CHCl_3$): 2929, 1703, 1392, 1082 cm^{-1}. Melting point: 102-104 °C.

(3*S*,5*S*,6*S*,8*R*,9*S*,10*R*,13*S*,14*S*,17*S*)-Hexadecahydro-17-((*S*)-2-hydroxy-6-methylhept-6-en-2-yl)-10,13-dimethyl-1*H*-cyclopenta[*a*]phenanthrene-3,6-diol. To a stirred suspension of magnesium turnings (80 mg, 3.3 mmol) in anhydrous diethyl ether (3.0 mL) was added 5-bromo-2-methyl-1-pentene (134 mg, 0.82 mmol). After stirring under reflux for 30 min, the initially produced Grignard reagent was added to the protected bis(*tert*-butyldimethylsilyl) ketone **5** (150 mg, 0.27 mmol) in anhydrous THF (2.0 mL) and left under reflux for an additional 30 min. The mixture was cooled in an ice bath and quenched with saturated NH_4Cl. The solution was extracted with diethyl ether (15 mL x 3). The organic layers were combined and washed with saturated NaCl, dried over Na_2SO_4 and evaporated in vacuo to afford a residue, which was subjected to column chromatography on silica gel. Elution with hexane-diethyl ether (4:1 v/v) afforded the bis(*tert*-butyldimethylsilyloxy) alcohol **6** (94.8 mg, 55%) as a white powder. This alcohol **6** was dissolved in 6.0 mL THF/CH_3CN (1:1 v/v) and treated with HF/pyridine (0.15 mL). After stirring for 1 h at 20 °C, the reaction was treated with water and extracted three times with diethyl ether (3 x 5 mL). The combined organic layers were washed with saturated

$NaHCO_3$ followed by saturated NaCl. The organic phases were collected, dried over Na_2SO_4 and concentrated in vacuo to give an oil. Flash column chromatography of this residue (silica gel, 5% methanol/95% diethyl ether) yield the desired triol **Oxy49** (49 mg, 80%). ^{1}H NMR ($CDCl_3$, 500 MHz) δ: 4.70 – 4.67 (2H, m), 3.58 (1H, dddd, *J* = 11.2, 11.2, 4.4, 4.4 Hz), 3.42 (1H, ddd, *J* = 10.8, 10.8, 4.4 Hz), 1.98 – 1.70 (10H, m), 1.71 (3H, s), 1.45 – 1.31 (10H, m), 1.25 (3H, s), 1.19 – 0.88 (10H, m), 0.86 (3H, s), 0.82 (3H, s). ^{13}C NMR ($CDCl_3$, 125 MHz) δ: 145.7, 109.9, 72.4, 70.9, 57.6, 56.2, 53.5, 48.6, 43.4, 42.9, 40.0, 38.1, 37.4, 37.1, 36.5, 33.4, 32.1, 31.0, 29.6, 26.2, 23.6, 22.3, 22.2, 22.1, 21.2, 13.6, 13.3. FTIR ($CHCl_3$): 3399, 2925, 1372, 739 cm^{-1}.

Animals

Fifty nine 8 week old male Lewis rats were purchased from Charles River Laboratories (Wilmington, MA) and were housed and maintained at the UCLA vivarium under the care of veterinarians and according to the regulations set forth by the UCLA Office of Protection of Research Subjects. All animals were euthanized using a standard CO_2 chamber 9 weeks after the spinal fusion procedure, and their spines were excised and fixed in buffered formalin for 24 hours before being stored in 40% ethyl alcohol.

Surgical procedures

Animals were anesthetized with 2% isoflurane administered in oxygen (1 L/min) and the surgical site was shaved and disinfected with alternative Betadine and 70% ethanol. Animals were premedicated with 0.15-mg buprenorphine and after surgery received tapered doses every 12 hours for 2 days. The posterolateral intertransverse process spinal fusion at L4–L5 in the rat is a well established model [Miyazake and Morishita et al, 2008; Miyazake and Sugiyama et al, 2008; Alanay et al, 2008]. The iliac crest was used as a landmark to locate the body of the L6 vertebra. A 4-cm longitudinal midline incision was made through the skin and subcutaneous

tissue over L4–L5 down to the lumbodorsal fascia. Then a 2-cm longitudinal paramedial incision was made in the paraspinal muscles bilaterally. The transverse processes of L4–L5 were exposed, cleaned of soft tissue, and decorticated with a high-speed burr. The surgical site was then irrigated with sterile saline, and 5x5x13 mm pieces of collagen sponge (Helistat, Integra Life Sciences, Plainsboro, NJ) containing dimethyl sulfoxide (DMSO) control, rhBMP2, or oxysterol were placed bilaterally, taking care to apply the implant to fully cover the transverse processes. The paraspinal muscles were then allowed to cover the implants and the lumbodorsal fascia and skin were closed with 4 – 0 Prolene sutures (Ethicon Inc., Somerville, NJ). Animals were allowed to ambulate, eat, and drink ad libitum immediately after surgery.

Radiographic analysis

Posteroanterior radiographs were taken on each animal at 4, 6, and 8 weeks post-surgery using an AMX-3 portable radiograph instrument (GE Healthcare, Piscataway, NJ). Radiographs were evaluated blindly by 3 independent observers employing the following standardized scale: 0: no fusion; 1: incomplete fusion with bone formation present; and 2: complete fusion. The scores from the observers were added together and a score of 5 or 6 was considered as complete fusion.

Manual assessment of fusion

Nine weeks after surgery, animals were euthanized and the spines were surgically removed and evaluated by 3 blinded independent observers for intersegmental motion. Any motion on either side between the facets or transverse processes, including unilateral movement, was considered nonunion (incomplete fusion). The bilateral absence of movement was considered complete fusion. Spines were scored as either fused or not fused. Unanimous agreement was required to consider a spine completely fused.

Micro-Computed Tomography

The explanted spines were subsequently scanned using high resolution micro-computed tomography (micro-CT), using a SkyScan 1172 scanner (SkyScan, Belgium) with a voxel isotropic resolution of 20 microns and an x-ray energy of 55 kVp and 167 mA to further assess the fusion rate and observe the fusion mass. 450 projections were acquired over an angular range of 180º with steps of 0.4 with an exposure time of 205 msec/slice. 10 frames were averaged at each rotation step to get better signal to noise ratio. A 0.5 mm aluminum filter was used to narrow down the x-ray beam frequency in order to minimize beam hardening artifact. Virtual image slices were reconstructed using the cone-beam reconstruction software version 2.6 based on the Feldkamp algorithm (SkyScan). These settings produced serial cross-sectional 1024 x 1024 pixel images. Sample re-orientation and 2D visualization were performed using DataViewer (SkyScan). 3D visualization was performed using Dolphin Imaging version 11 (Dolphin Imaging & Management Solutions, Chatsworth, CA). Fusion was defined as the bilateral presence of bridging bone between the L4 and L5 transverse processes. The reconstructed images were judged to be fused or not fused by 3 experienced independent observers and only a consensus was considered fused.

Histology

After the rats were sacrificed, the spines (L3-L5) were surgically extracted and the specimens were fixed as described earlier. Two representative specimens from each experimental group were processed undecalcified by dehydration, clearing in xylene and embedding in methyl methacrylate as we have previously reported [Pereira et al, 2007]. Serial coronal sections 5 µm thick were cut and selected slides were stained with toluidine blue pH 6.4. Photomicrographs of sections were obtained as previously reported using a ScanScope XT System (Aperio

Technologies, Inc., Vista, CA, USA) at a magnification of X10 in Figure 7A and X20 in Figure 7B [Magyar et al, 2008]. Fusion was defined as bony trabeculae bridging from one transverse process to the next.

Statistical Analysis

Statistical analyses were performed using the StatView 5 program. All p values were calculated using ANOVA and Fisher's projected least significant difference (PLSD) significance test. A value of $p < 0.05$ was considered significant.

Results

Novel oxysterols induce osteogenic differentiation of bone marrow stromal cells – To develop a therapeutically useful oxysterol for inducing osteogenesis, we modified the molecular structure of 20(*S*)-hydroxycholesterol (20S), the most potent osteogenic naturally occurring oxysterol that we had previously identified [Kha et al, 2004; Kim et al, 2010]. As we previously reported, the combination of 20S and 22(*S*)- or 22(*R*)-hydroxycholesterol was necessary in order to achieve robust osteogenic differentiation of pluripotent mesenchymal cells *in vitro* as compared to using 20S alone [Kha et al, 2004]. However, we were interested in creating, if possible, a molecule(s) that could be used as a single agent to induce the differentiation of osteoprogenitor cells into mature osteoblastic cells for future therapeutic development and use in indications that would benefit from increased bone formation such as local indications (for example, spinal fusion and fracture healing) and systemic indications (for example, osteoporosis). From a collection of more than 40 oxysterol analogs that were synthesized, two molecules, Oxy34 and Oxy49 (Figure 1A), were selected for further study based on their relative potencies in inducing ALP activity in multipotent murine bone marrow stromal cells (MSC), M2-10B4 (M2). The differences between the molecular structures of 20S vs. Oxy34 and Oxy49 are the addition of a hydroxyl (OH) group to carbon 6 (C6) in both Oxy34 and Oxy49, and the addition of a double bond between C25 and C27 in Oxy49 (Figure 1). Oxy34 or Oxy49 treatment for 48 hours caused a dose-dependent induction of the early osteogenic differentiation marker ALP activity, with an EC50 of approximately 800 nM for Oxy34 and 900 nM for Oxy49 (Figure 1B, C). By comparison, the EC50 for 20S was approximately 5 μM and in combination with 22S at a 1:1 molar ratio was about 600 nM (data not shown).

Next we examined the ability of Oxy34 and Oxy49 to induce the expression of Runx2 and its target gene Osterix (Osx), both early markers and transcriptional regulators of osteogenic differentiation [Franceschi et al, 2007; Zhou et al, 2010]. Treatment of M2 cells for 48 hours with 5 μM Oxy34 or Oxy49 induced a small but significant increase in Runx2 mRNA expression by 1.5-2 fold (data not shown) and a robust induction of Osx expression by more than 8 fold (Figure 2A). The small effect of oxysterols on Runx2 mRNA expression is consistent with our previous finding that the stimulatory effect of the naturally occurring osteogenic oxysterol combination 20S+22S on Runx2 is primarily at a post-transcriptional level as suggested by the induced DNA binding activity of Runx2 in oxysterol-treated cells with minimal effects on Runx2 mRNA or protein levels [Richardson et al, 2007]. Formation of fully mature osteoblastic cells in M2 cultures treated with Oxy34 and Oxy49 was further assessed by measuring the mRNA expression of ALP, as well as the later osteogenic differentiation markers bone sialoprotein (BSP) and osteocalcin (OCN). The formation of a mineralized extracellular matrix was measured to assess osteoblast function. Treatment of M2 cells for 7 days with Oxy34 or Oxy49 caused a significant increase in the expression of ALP, BSP and OCN expression (Figure 2B, C, D), and treatment for 14 days resulted in robust mineralization (Figure 2E). Similar results were found when using C3H10T1/2 multipotent embryonic fibroblasts (data not shown).

Oxy34 and Oxy49 induce osteogenic differentiation through activation of Hedgehog pathway signaling – To determine whether similar to the parent osteogenic oxysterols [Dwyer et al, 2007], Oxy34 and Oxy49 induce osteogenic differentiation of MSC through activation of Hh pathway signaling, we first measured the expression of Hh target genes Patched 1 (Ptch1), Gli1, and Hedgehog-interacting protein (HIP) in response to Oxy34 and Oxy49. Treatment of M2 cells for 48 hours with 5 μM Oxy34 or Oxy49 induced the expression of all three Hh target

genes which were blocked by the specific Hh pathway inhibitor, cyclopamine (Figure 3A). Activation of the Hh pathway by Oxy34, Oxy49, and the positive control recombinant human sonic hedgehog (Shh) was further demonstrated in M2 cells transfected with an 8X-Gli luciferase reporter (Figure 3B).

The role of Hh signaling in Oxy34- and Oxy49-induced osteogenic differentiation of M2 cells was confirmed by the ability of cyclopamine to completely block the induction of the osteogenic differentiation markers ALP activity (data not shown) and ALP, BSP, and OCN mRNA expression by these oxysterols (Figure 2B,C,D).

Oxy34 and Oxy49 inhibit adipogenic differentiation of bone marrow stromal cells – We previously reported that osteogenic oxysterols inhibit adipogenic differentiation of multipotent mesenchymal cells and MSC through Hh signaling-mediated inhibition of the master regulator of adipogenesis, PPARγ. (Ref) To determine whether Oxy34 and Oxy49 inhibit adipogenic differentiation of MSC, M2 cells were treated with the PPARγ ligand troglitazone (Tro), which induces adipogenesis in M2 cells, in the presence or absence of Oxy34 or Oxy49. Results showed that both oxysterols completely inhibited Tro-induced expression of PPARγ and the adipogenic differentiation markers lipoprotein lipase (LPL) and adipocyte fatty acid binding protein (aP2) (Figure 4A). Similarly, 10 day cultures showed robust Tro-induced adipocyte formation as indicated by Oil Red O staining, which was completely blocked by Oxy34 and Oxy49 (Figure 4B, C).

Oxy34 and Oxy49 stimulate bone formation and spinal fusion in vivo

Mature Lewis rats at 8 weeks of age (Charles River, Wilmington, MA) were divided into 6 treatment groups for posterolateral spinal fusion. Each treatment group received collagen sponge implants containing different reagents, as follows: Group I – control vehicle only (n=9), Group II

– 5 μg rhBMP-2 (n=10), Group III – 0.2 mg Oxy34 (n=10), Group IV – 2 mg Oxy34 (n=10), Group V – 20 mg Oxy34 (n=10), and Group VI – 20 mg Oxy49 (n=10). These animals were followed for nine weeks post operatively and then euthanized. Various methods were used to determine bone formation and spinal fusion, as described below.

Radiographical analysis

Radiographs of the rat spines were obtained at 4, 6 and 8 weeks postoperatively. At 4 weeks, the spines of rats in Groups II (BMP2) , IV (2 mg Oxy34), V (20 mg Oxy34), and VI (20 mg Oxy49) began to show evidence of bone formation between the L4 and L5 transverse processes and bony bridging was detected in some animals in Groups II, V and VI. At 6 weeks there was an increase in bone formation and consolidation of the fusion mass in Groups II, IV, V and VI. No bone formation was seen in Groups I (control) and III (0.2 mg Oxy34). At 8 weeks bilateral bridging bone formation and fusion was seen in 8/10 animals in Group II, 3/10 in group IV, 8/10 in Group V, and 8/10 in Group VI. Additionally unilateral bridging bone was seen in the 2 remaining animals in Groups II, IV, and V. No significant bone formation was seen in Groups I and III at 8 weeks. Representative radiographs from 2 animals in each group are shown in Figure 5. It is clear that bone formation and rate of fusion increased dose-dependently in animals treated with Oxy34.

Manual assessment and gross evaluation of bone formation

Each specimen was evaluated by 3 independent observers, and all observers were in agreement on all specimens. All specimens from Groups I (control) and III (0.2 mg Oxy34) had significant intersegmental movement and were designated as non-fused. All spines from Groups II (BMP2), V (20 mg Oxy34), and VI (20 mg Oxy49) were assessed as fused. In Group IV (2 mg Oxy34) 5

out of 10 specimens were fused. The amount of bone mass was less in Group IV than that seen in Groups II, V and VI.

Micro-computed tomography and histological assessment

MicroCT analysis was performed on all excised spines. MicroCT is the most sensitive method of determining the presence of bone bridging the intertransverse process space. Complete fusion was defined as bridging bone between the transverse processes with no gap. Multiple cut sections were reconstructed to evaluate the presence of a bony bridge between the transverse processes. Bone bridging the transverse processes was observed in all samples graded as fused. There was no bone formation in the animals from Group I (Control). Although no fusions occurred in Group III (0.2 mg Oxy34) there were several specimens with some modest bone formation. Groups II (BMP2), V (20 mg Oxy34), and VI (20 mg Oxy49) resulted in 8 bilateral and 2 unilateral fusions in a total of 10 animals. In Group IV (2 mg Oxy34) 3 out of 10 spines exhibited bilateral fusion and 2 unilateral fusion. Those with unilateral fusions in groups II, V and VI also had significant bone formation on the side that was incompletely fused with only a small gap in between the bridging bone mass in the intertransverse process space, but since there was still a gap, it was graded as not fused. This demonstrates the sensitivity of MicroCT to determine fusion even when there is no intersegmental motion.

Histological assessment of two specimens from each group demonstrated the formation of trabecular bone within the fusion mass and continuous cortical bone connecting the transverse processes of the fully fused lumbar vertebrae in rats treated with BMP2 (Group II), or with the 2 or 20 mg dose of Oxy34 (Groups IV and V, respectively) and 20 mg of Oxy49 (Group VI) (Figure 7A). Bone formation was not present in specimens from control rats (Group I, Figure 7) and those treated with 0.2 mg of Oxy34 (Group III, data not shown). Although the relative

abundance of trabecular and cortical bone was similar in rats treated with BMP2 or 20 mg of Oxy34 or Oxy49, visual inspection of the histological specimens indicated that BMP2 also induced the abundant formation of adipocytes within the fusion mass, whereas adipocytes within the fusion mass of oxysterol-treated rats seemed significantly less than that in the BMP2-treated rats (Figure 7B).

Discussion

The use of osteoinductive materials to enhance bone healing is of critical importance for management of patients with orthopaedic injuries. This is especially true in patients undergoing complicated spinal fusion procedures, fracture non-union revisions (i.e. fractures that fail to completely heal after a prior attempt at inducing fusion and require re-operation), and in patients with co-morbidities such as diabetes and osteoporosis that impair their healing potential. Historically this has been achieved through the use of autogenous bone grafting or by using the potent osteogenic factors, rhBMP2 and rhBMP7. While these strategies are effective in stimulating bone formation and inducing spinal fusion, they are also associated with significant complications and considerable financial costs that hinder their use. Common complications of BMP use in bone fusion procedures include ectopic bone formation, inflammatory responses, and transient resorption of vertebral bodies [Hsu and Wang, 2008; Axelrod and Einhorn, 2009; Chen et al, 2010; Garrett et al, 2010; Shahlaie and Kim, 2008; Bieniasz et al, 2009; Langenfeld et al, 2003; Gordon et al, 2009]. Such limitations have established the continued need for identification of new strategies to stimulate bone formation in a safe and cost-effective manner.

During the past few years, we have identified and characterized naturally occurring oxysterols that stimulate the osteogenic differentiation of osteoprogenitor cells and stimulate bone formation in vivo [Kha et al, 2004; Richardson et al, 2007; Amantea et al, 2008; Aghaloo et al, 2007]. In this report we present data regarding two novel small molecule oxysterols, Oxy34 and Oxy49 that were designed and synthesized by our group, and we demonstrate their potent osteogenic effects in vitro and in vivo. Similar to their naturally occurring analogues [Dwyer et al, 2007; Kim et al, 2007], Oxy34 and Oxy49 mediate osteogenic differentiation of cells through activation of Hh signaling and inhibit adipogenic differentiation of progenitor cells. Given that

the relative effectiveness of Oxy34 and Oxy49 is comparable to that of rhBMP2, but the cost of producing them is significantly less, we suggest that small molecule osteogenic oxysterols may be excellent candidates for development into the next generation of osteogenic compounds for stimulation of localized bone formation such as in spinal fusion and fracture repair. Although the effectiveness of stimulating osteogenesis using 20 mg of oxysterols in our rat spinal fusion model was comparable to that induced by 5 μg of rhBMP2, it is difficult to compare the relative doses of these molecules given the fact that the former are small molecule lipids with molecular weights of 420 and 418 grams/mole for Oxy34 and Oxy49 respectively, and the latter is a large protein that consists of 115 amino acids with an apparent molecular weight of 26 kDa [Heng et al, 2010]. In future studies we will determine whether by further increasing the dose of oxysterols, the relative amount of bone formed and/or the rate of fusion can be further enhanced.

Although microCT and histological analysis of the fusion masses induced by rhBMP2 and oxysterols demonstrated quantitatively and qualitatively comparable bone formation, including the presence of trabeculae and cortical bone, we recognized an apparent difference between the relative abundance of adipocytes in the fusion mass from BMP2 vs. oxysterol treated rats even though we did not statistically quantify the actual number of adipocytes in the fusion masses due to the limited number of specimens prepared for histological analysis. In a previous rat spinal fusion study we had similarly observed a large number of adipocytes forming in the fusion mass induced by 5 μg BMP2 [Parhami and Wang, 2010, unpublished observations]. Consistent with our in vivo findings, in vitro pro-adipogenic effects of BMP2 have been reported [Sottile and Seuwen, 2000; Chen et al, 1998; Zehentner et al, 2000]. In contrast, we previously demonstrated the anti-adipogenic effects of osteogenic oxysterols that are also mediated through activation of Hh signaling [Kha et al, 2004; Kim et al, 2007]. Although the significance of the

large numbers of adipocytes in the fusion mass induced by BMP2 is not known at this time, we speculate that the presence of fat in the bony tissue may have adverse effects on the quality and strength of bone that is formed. In addition, since osteoblasts and adipocytes arise from the same mesenchymal progenitor cells [Nuttall and Gimble, 2004, Pei and Tontonoz, 2004], it is plausible that adipocyte formation occurs at the expense of osteoblasts in the fusion mass. In that case, the apparent lower prevalence of adipocytes in the fusion mass induced by oxysterols may allow for a greater number of osteoblasts to form that would ultimately enhance bone formation and the fusion process. Moreover, we speculate that co-administration of osteogenic oxysterols with BMP2 could inhibit the adipogenic effects of BMP2 and ultimately improve the induction of new bone, possibly at reduced concentrations of BMP2. Consistent with this possibility, we have found that osteogenic oxysterols do inhibit BMP2-induced adipogenesis of multipotent bone marrow stromal cells and enhance its osteogenic potency in vitro (Parhami et al. unpublished observations). These observations further support the continued investigation of osteogenic oxysterols as potential therapeutic agents for bone repair.

Acknowledgements

This work was supported by NIAMS/NIH Grant RO1AR050426 and in part by a sponsored research award from Fate Therapeutics, Inc. (San Diego, CA. USA).

Figure Legends

Figure 1. *Synthetic oxysterol small molecules with osteogenic properties.* (A) The molecular structures of Oxy34, Oxy49 and 20(*S*)-hydroxycholesterol (20S) are shown. Oxy34 is different from 20S in having an extra OH group on C6. Oxy49 has an extra OH group on C6 similar to Oxy34 as well as a double bond between C25 and C27. Synthesis of Oxy34 and Oxy49 are described in the Methods section. (B) M2-10B cells at confluence were treated with vehicle or 0.25-10 μM of Oxy34 or Oxy49. After 4 days, alkaline phosphatase (ALP) activity was measured in whole cell extracts. Data from a representative of 3 separate experiments are reported as the mean ± SD of triplicate determinations, normalized to protein concentration ($p<0.01$ for cells treated with all concentrations above 0.5 μM of Oxy34 and Oxy49 vs. control vehicle treated cells).

Figure 2. *Induction of osteogenic differentiation markers by Oxy34 and Oxy49*. M2-10B4 cells at confluence were pretreated with control vehicle or 4 μM cyclopamine (Cyc) for 2 hours. Next, 5 μM oxysterol or control vehicle were added to control or Cyc treated cells as shown. (A) mRNA expression for Osterix (Osx) after 48 hours, and (B, C, D) mRNA expression for bone alkaline phosphatase (ALP), bone sialoprotein (BSP), and osteocalcin (OCN) after 6 days of treatment with oxysterols were measured using Q-RT-PCR. Results from a representative experiment are reported as the mean of triplicate determinations ± SD ($p<0.001$ for control vs. oxysterol treatment and for oxysterol vs. oxysterol+Cyc treatment groups for all genes shown). (E) ^{45}Ca incorporation assay after 14 days of treatment with oxysterols was performed in order to quantify induction of extracellular matrix mineralization. Results from a representative experiment are reported as the mean of quadruplicate determinations ± SD ($p<0.001$ for control vs. all oxysterol treated conditions).

Figure 3. *Activation of Hedgehog pathway signaling by Oxy34 and Oxy49***.** (A) M2-10B4 cells at confluence were pretreated with control vehicle or 4 μM cyclopamine (Cyc) for 2 hours. Next, 5 μM oxysterol or control vehicle were added to control or Cyc treated cells as shown. mRNA expression for Hh pathway target genes Ptch1, Gli1, and HIP after 48 hours of treatment with oxysterols is shown. Results from a representative experiment are reported as the mean of triplicate determinations ± SD (p<0.001 for control vs. oxysterol treatment and for oxysterol vs. oxysterol+Cyc treatment groups for all genes shown). (B) M2-10B4 cells at 70% confluence were transiently transfected with a Gli1 overexpression vector, a Gli response element reporter construct (pGL3b-8xGli-Luciferase) or pGL3b-Luciferase plasmid in combination with pTK-Renilla-Luciferase plasmid. Luciferase activity was measured after 48 hrs of treatment with 5 μM oxysterols or 400 ng/ml recombinant human Shh, and normalized for transfection efficiency using the Renilla luciferase activity. Data are reported as the mean of triplicate determinations ± SD (p<0.001 for control vs. Oxy34, Oxy49, and Shh for pGL3b-8XGli).

Figure 4. *Inhibition of adipogenesis by Oxy34 and Oxy49.* (A) M2-10B4 cells were treated with control vehicle, 10 mM Troglitazone (Tro), or 5 mM Oxy34 or Oxy49, alone or in combination as demonstrated. After 72 hours, mRNA expression for PPAR gamma, lipoprotein lipase (LPL), and adipocyte fatty acid binding protein (aP2) were measured using Q-RT-PCR Results from a representative experiment are reported as the mean of triplicate determinations ± SD (p<0.001 for control vs. Tro and for Tro vs. Tro+Oxy34 and Tro+Oxy49 for all genes shown). (B) In parallel cultures to those described in (A), after 10 days of treatment adipocyte formation was examined by Oil Red O staining (Phase contrast x100), and quantified by light microscopy in triplicate wells (C). Results from a representative experiment are shown as the mean of 5

random fields per triplicate wells per condition ± SD (p<0.001 for control vs. Tro and for Tro vs. Tro+Oxy34 and Tro+Oxy49).

Figure 5. *Radiographic analysis of the effect of oxysterols and rhBMP2 on spinal fusion.* Faxitron images of 2 animals from the indicated groups at 8 weeks postoperatively are shown**.** Group I (Control); arrows demonstrate the intertransverse process space with no bone formation. Group II (BMP2); arrows demonstrate bilateral fusion at L4-5. Group V (Oxy34-20mg); arrows demonstrate bridging bone mass and bilateral fusion at L4-5. Group VI (Oxy49-20mg); arrows demonstrate bridging bone mass and bilateral fusion at L4-5.

Figure 6. *MicroCT analysis of the effect of oxysterol and rhBMP on spinal fusion.* Micro CTs of 2 animals from the indicated groups are shown. Group I (Control); arrows indicate the intertranverse process space with no bone formation. Group II (BMP2); arrows indicate bone mass bridging the intertransverse process space and bilateral fusion at L4-5. Group V (Oxy34-20mg); arrows indicate bone mass bridging the intertransvers process space and bilateral fusion at L4-5. Group VI (Oxy49-20mg); arrows indicate bone mass bridging the intertransverse process space and bilateral fusion at L4-5.

Figure 7. *Histological analysis of the effect of oxysterols on spinal fusion.* (A) Coronal histological sections of 2 separate animals from each group are shown (magnification X10). Group I (Control) has no significant bone formation at the intertransverse process space (arrows) . Group II (BMP2) demonstrates bridging bone at L4-L5 (arrows) with clear evidence of trabecular and cortical bone forming the fusion mass. Group V (Oxy34-20mg) and Group VI (Oxy49-20mg) specimens demonstrate significant bone formation at the intertransverse process space (arrows) with trabecular and cortical bone formation comparable to that induced by BMP2. (B) Coronal histological sections from 2 animals each in Groups II (BMP2) and Group VI

(Oxy49-20mg) demonstrate significant adipocyte formation in the fusion mass of BMP2 treated animals and substantially fewer adipocytes in the fusion mass from oxysterol treated animals (arrows, magnification X20).

References

Aghaloo TL, Amantea CM, Cowan CM, Richardson JA, Wu BM, Parhami F, Tetradis S. 2007. Oxysterols enhance osteoblast differentiation in vitro and bone healing in vivo. J Orthop Res 25:1488-1497.

Alanay A, Chen C, Lee S, Murray SS, Brochmann EJ, Miyazaki M, Napoli A, Wang JC. 2008. The adjunctive effect of a binding peptide on bone morphogenetic protein enhanced bone healing in a rodent model of spinal fusion. Spine 33:1709-1713.

Amantea CM, Kim WK, Meliton V, Tetradis S, Parhami F. 2008. Oxysterol-induced differentiation of marrow stromal cells is regulated by Dkk-1 inhibitable and PI3-kinase mediated signaling. J Cell Biochem 105:424-436.

Arrington ED, Smith WJ, Chambers HG, Bucknell AL, Davino NA. 1996. Complications of iliac crest bone graft harvesting. Clin Orthop Relat Res 329:300-309.

Axelrad TW, Einhorn TA. 2009. Bone morphogenetic proteins in orthopaedic surgery. Cytokine & Growth Factor Rev 20:481-488.

Bessa PC, Casal M, Reis RL. 2008. Bone morphogenetic proteins in tissue engineering: the road from the laboratory to the clinic, part I (basic concepts). J Tissue Eng Regen Med 2:1-13.

Bieniasz M, Oszajca K, Eusebio M, Kordiak J, Bartkowiak J, Szemraj J. 2009. The positive correlation between gene expression of the two angiogenic factors: VEGF and BMP-2 in lung cancer patients. Lung Cancer 3:319-326.

Brown A, Stock G, Patel AA, Okafar C, Vaccaro A. 2006 Osteogenic protein-1: a review of its utility in spinal applications. BioDrugs 20:243-251.

Cahill KS, Chi JH, Day A, Claus EB. 2009. Prevalence, complications, and hospital charges

associated with use of bone-morphogenetic proteins in spinal fusion procedures. JAMA 302:58-66.

Chen D, Ji X, Harris MA, Feng JQ, Karsenty G, Celeste AJ, Rosen V, Mundy GR, Harris SE. 1998. Differential roles for bone morphogenetic protein (BMP) receptor type IB and IA in differentiation and specification of mesenchymal precursor cells to osteoblast and adipocyte lineages. J Cell Biol 142:295-305.

Chen NF, Smith ZA, Stiner E, Armin S, Sheikh H, Khoo LT. 2010. Symptomatic ectopic bone formation after off-label use of recombinant human bone morphogenetic protein-2 in transforaminal lumbar interbody fusion. J Neursurg Spine 12:40-46.

Dwyer JR, Sever N, Carlson M, Nelson SF, Beachy PA, Parhami F. 2007. Oxysterols are novel activators of the Hedgehog signaling pathway in pluripotent mesenchymal cells. J Biol Chem 282:8959-8968.

Franceschi RT. 2005. Biological approaches to bone regeneration by gene therapy. J Dent Res 84:1093-1103.

Franceschi RT, Ge C, Xiao G, Roca H, Jiang AD. 2007. Transcriptional regulation of osteoblasts. Ann NY Acad Sci 1116:196-207.

Garrett MP, Kakarla UK, Porter RW, Sonntag VK. 2010. Formation of painful seroma and edema after the use of recombinant human bone morphogenetic protein-2 in posterolateral lumbar spine fusion. Neurosurgery 66:1044-1049.

Habibovic P, de Groot K. 2007. Osteoinductive biomaterials – properties and relevance in bone repair. J Tissue Eng Regener Med 1:25-32.

Heng S, Paule S, Hardman B, Li Y, Singh H, Rainczuk A, Stephens AN, Nie G. 2010.

Posttranslational activation of bone morphogenetic protein 2 is mediated by proprotein convertase 6 during decidualization for pregnancy establishment. Endocrinology 151:3909-3917.

Gautschi OP, Frey SP, Zellweger R. 2007. Bone morphogenetic proteins in clinical applications. ANZ J Surg 77:626-631.

Glassman SD, Gum JL, Crawford CH, Shields CB, Carreon LY. 2010. Complications with recombinant human bone morphogenetic protein-2 in posterolateral spine fusion associated with a dural tear. Spine J 10 [Epub ahead of print].

Gordon KJ, Kirkbride KC, How T, Blobe GC. 2009. Bone morphogenetic proteins induce pancreatic cancer cell invasiveness through a Smad1-dependent mechanism that involves matrix metalloproteinase-2. Carcinogenesis 30:238-248.

Hsu WK, Wang JC. 2008. The use of bone morphogenetic protein in spine fusion. Spine J 8:419-425.

Ito H, Akiyama H, Shigeno C, Iyama K, Matsuoka H, Nakamura T. 1999. Hedgehog signaling molecules in bone marrow cells at the initial stage of fracture repair. Biochem Biophys Res Commun 262:443-451.

Johnson EE, Urist MR. 2000. Human bone morphogenetic protein allografting for reconstruction of femoral non-union. Clin Ortho 371:61-74.

Kha HT, Basseri B, Shouhed D, Richardson J, Tetradis S, Hahn TJ, Parhami F. 2004. Oxysterols regulate differentiation of mesenchymal stem cells: pro-bone and anti-fat. J Bone Miner Res 19:830-840.

Khosla S, Westerndorf JJ, Oursler MJ. 2008. Building bone to reverse osteoporosis and repair fractures. J Clin Invest 118:421-428.

Kim W, Meliton V, Amantea CM, Hahn TJ, Parhami F. 2007. 20(*S*)-hydroxycholesterol inhibits PPARγ expression and adipogenic differentiation of bone marrow stromal cells through a hedgehog-dependent mechanism. J Bone Miner Res 22:1711-1719.

Kim W, Meliton V, Bourquard N, Hahn TJ, Parhami F. 2010. Hedgehog signaling and osteogenic differentiation in multipotent bone marrow stromal cells are inhibited by oxidative stress. J Cell Biochem 111:1199-1209.

Kim W, Meliton V, Tetradis S, Weinmaster G, Hahn TJ, Carlson M, Nelson SF, Parhami F. 2010. Osteogenic oxysterol, 20(*S*)-hydroxycholesterol, induces Notch target gene expression in bone marrow stromal cells. J Bone Miner Res 25:782-795.

Langenfeld EM, Calvano SE, Abou-Nukta F, Lowry SF, Amenta P, Langenfeld J. 2003. The mature bone morphogenetic protein-2 is aberrantly expressed in non-small cell lung carcinomas and stimulates tumor growth of A549 cells. Carcinogenesis 24:1445-1454.

Lipson SJ. 2004. Spinal-fusion surgery-advances and concerns. N Engl J Med 350:643-644.

Lum L, Beachy PA. 2004. The hedgehog response network: sensors, switches, and routers. Science 304:1755-1759.

Magyar CE, Aghaloo TL, Atti E, Tetradis S. 2008. Ostene, a new alkylene oxide copolymer bone hemostatic material, does not inhibit bone healing. Neurosurgery 63:ONS373-ONS378.

Miyaji T, Nakase T, Iwasaki M, Kuriyama K, Tamai N, Higuchi C, Myoui A, Tomita T, Yoshikawa H. 2003. Expression and distribution of transcripts for sonic hedgehog in the early phase of fracture repair. Histochem Cell Biol 119:233-237.

Miyazaki M, Morishita Y, He W, Hu M, Sintuu C, Hymanson HJ, Falakassa J, Tsumura H,

Wang JC. 2008. A porcine collagen-derived matrix as a carrier for recombinant human bone morphogenetic protein-2 enhances spinal fusion in rats. Spine J 9:22-30.

Miyazaki M, Sugiyama O, Tow B, Zou J, Morishita Y, Wei F, Napoli A, Sintuu C, Lieberman JR, Wang JC. 2008. The effects of lentiviral gene therapy with bone morphogenetic protein-2-producing bone marrow stromal cells on spinal fusion in rats. J Spinal Disord Tech 21:372-379.

Miyazaki M, Tsumura H, Wang JC, Alanay A. 2009. An update on bone substitutes for spinal fusion. Eur Spine J 18:783-799.

Mundy GR. 2002. Directions of drug discovery in osteoporosis. Annu Rev Med 53:337-354.

Nuttall ME, Gimble JM. 2004. Controlling the balance between osteoblastogenesis and adipogenesis and the consequent therapeutic implications. Curr Opin Pharmacol 4:290-294.

Pei L, Tontonoz P. 2004. Fat's loss is bone's gain. J Clin Invest 113:805-806.

Pereira RC, Stadmeyer LE, Smith DL, Rydziel S, Canalis E. 2007. CCAAT/Enhancer-binding protein homologous protein (CHOP) decreases bone formation and causes osteopenia. Bone 40:619-626.

Richardson JA, Amantea CM, Kianmahd B, Tetradis S, Lieberman JR, Hahn TJ, Parhami F. 2007. Oxysterol-induced osteoblastic differentiation of pluripotent mesenchymal cells is mediated through a PKC- and PKA-dependent pathway. J Cell Biochem 100:1131-1145.

Rihn JA, Kirkpatrick K, Albert TJ. 2010. Graft options in posterolateral and posterior interbody lumbar fusion. Spine 35:1629-1639.

Rodan GA, Martin TJ. 2002. Therapeutic approaches to bone diseases. Science 289:1508-1514.

Shahlaie K, Kim KD. 2008. Occipitocervical fusion using recombinant human bone morphogenetic protein-2. Spine 33:2361-2366.

Simpson F, Kerr MC, Wicking C. 2009. Trafficking, development and hedgehog. Mech Dev 126:279-288.

Sottile V, Seuwen K. 2000. Bone morphogenetic protein-2 stimulates adipogenic differentiation of mesenchymal precursor cells in synergy with BRL 49653 (rosiglitazone). FEBS Lett 475:201-204.

Vaccaro AR, Chiba K, Heller JG, Patel TC, Thalgott JS, Truumees E, Fischgrund JS, Craig MR, Berta SC, Wang JC. 2002. Bone grafting alternatives in spinal surgery. Spine J 2:206-215.

Varjosalo M, Taipale J. 2008. Hedgehog: functions and mechanisms. Genes Dev 22:2454-2472.

Yoon ST, Boden SD. 2002. Osteoinductive molecules in orthopaedics: Basic science and preclinical studies. Clin Orthop and Rel Res 395:33-43.

Zehentner BK, Leser U, Burtscher H. 2000. BMP-2 and sonic hedgehog have contrary effects on adipocyte-like differentiation of C3H10T1/2 cells. DNA & Cell Biol 19:275-281.

Zhou X, Zhang Z, Feng JQ, Dusevich VM, Sinha K, Zhang H, Darnay BG, de Crombrugghe B. 2010. Multiple functions of Osterix are required for bone growth and homeostasis in postnatal mice. Proc Natl Acad Sci 107:12919-12924.

Zhu W, Rawlins BA, Boachie-Adjei O, Myers ER, Arimizu J, Choi E, Lieberman JR, Crystal

RG, Hidaka C. 2004. Combined bone morphogenetic protein-2 and -7 gene transfer enhances osteoblastic differentiation and spine fusion in a rodent model. J Bone Miner Res 19:2021-2032.

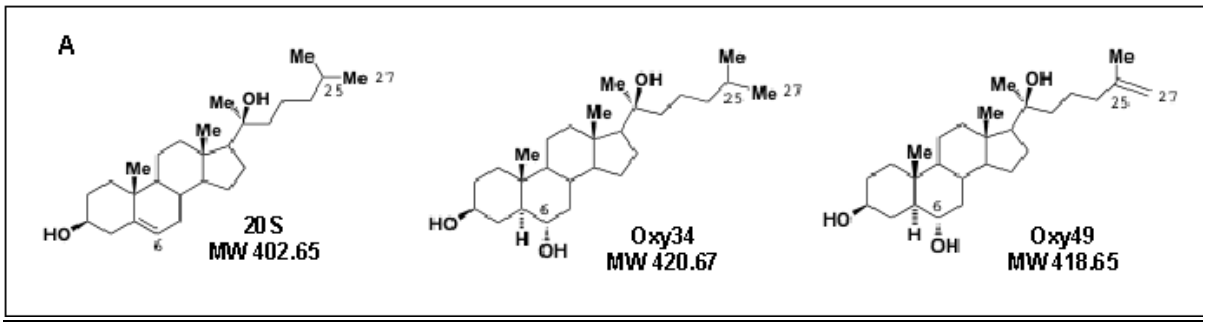

Figure 1A

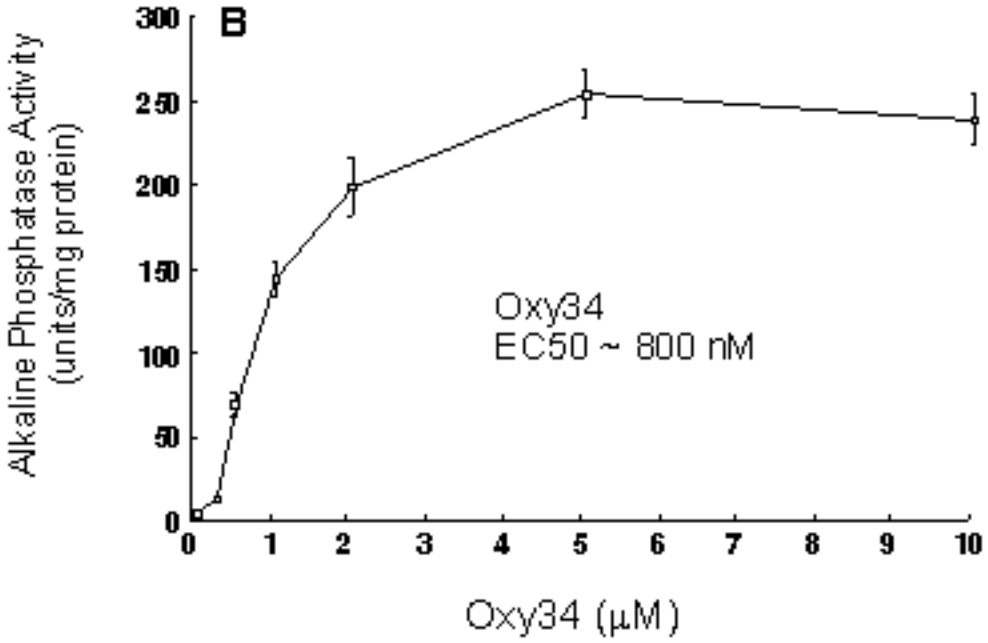

Figure 1B

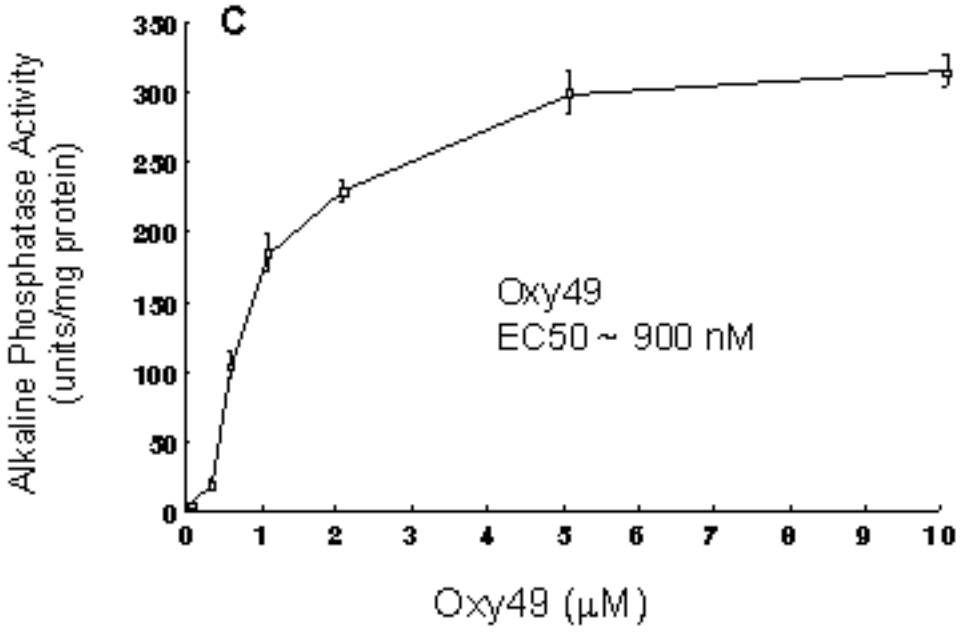

Figure 1C

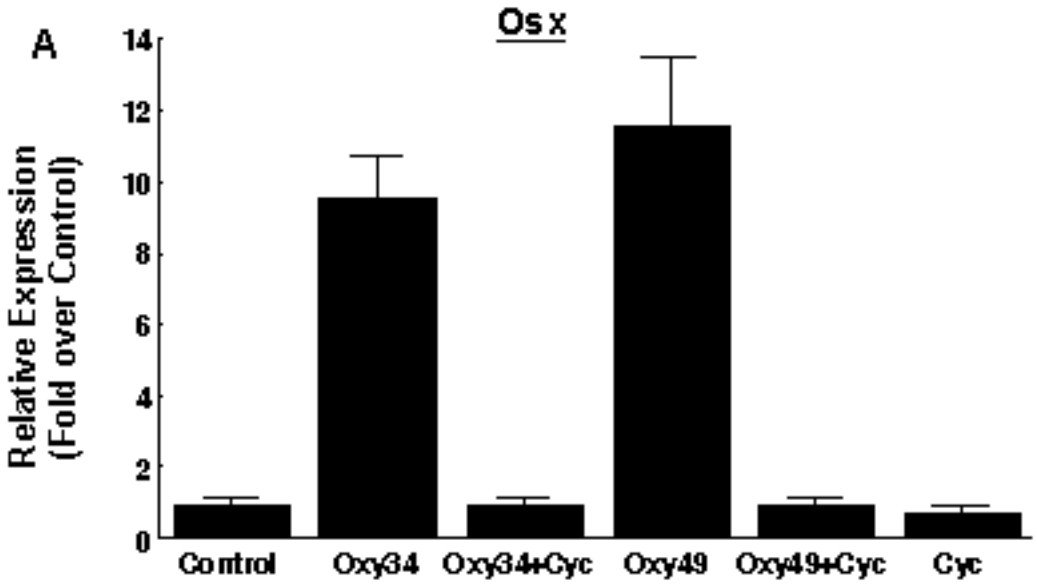

Figure 2A

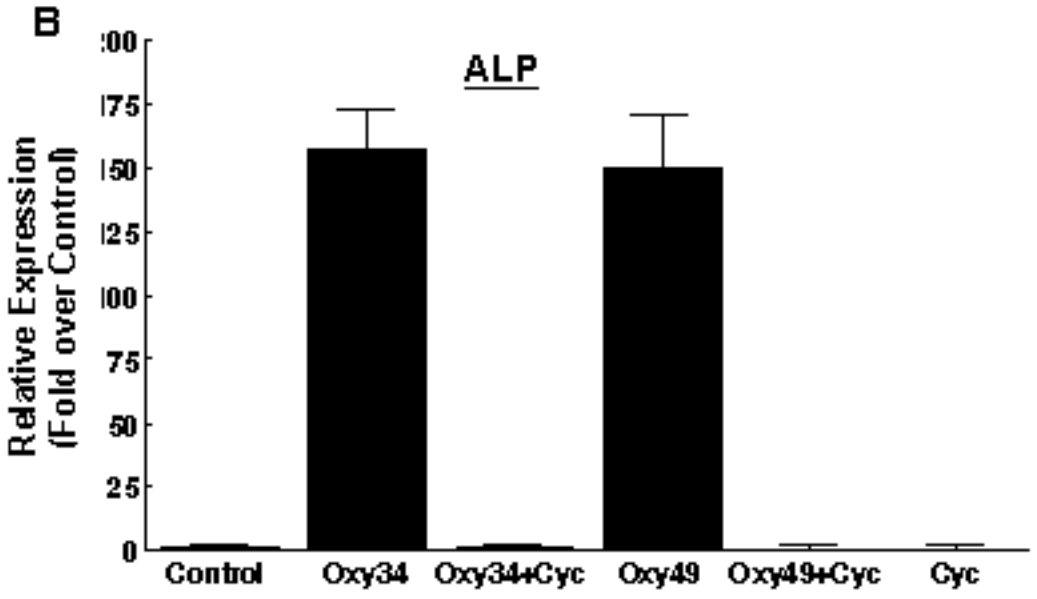

Figure 2B

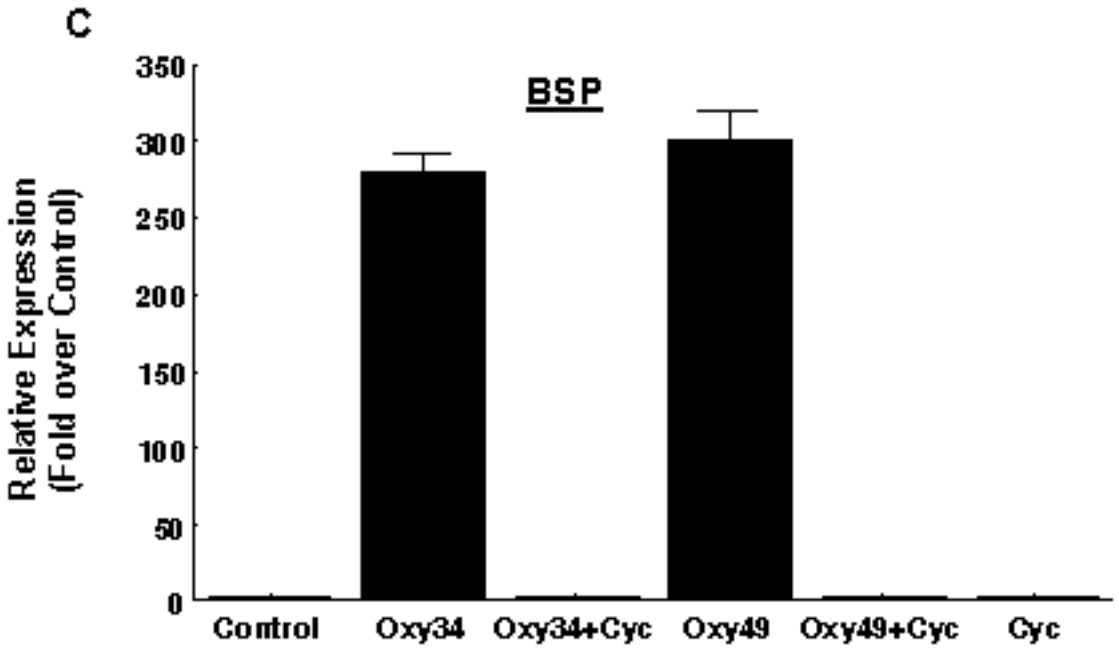

Figure 2C

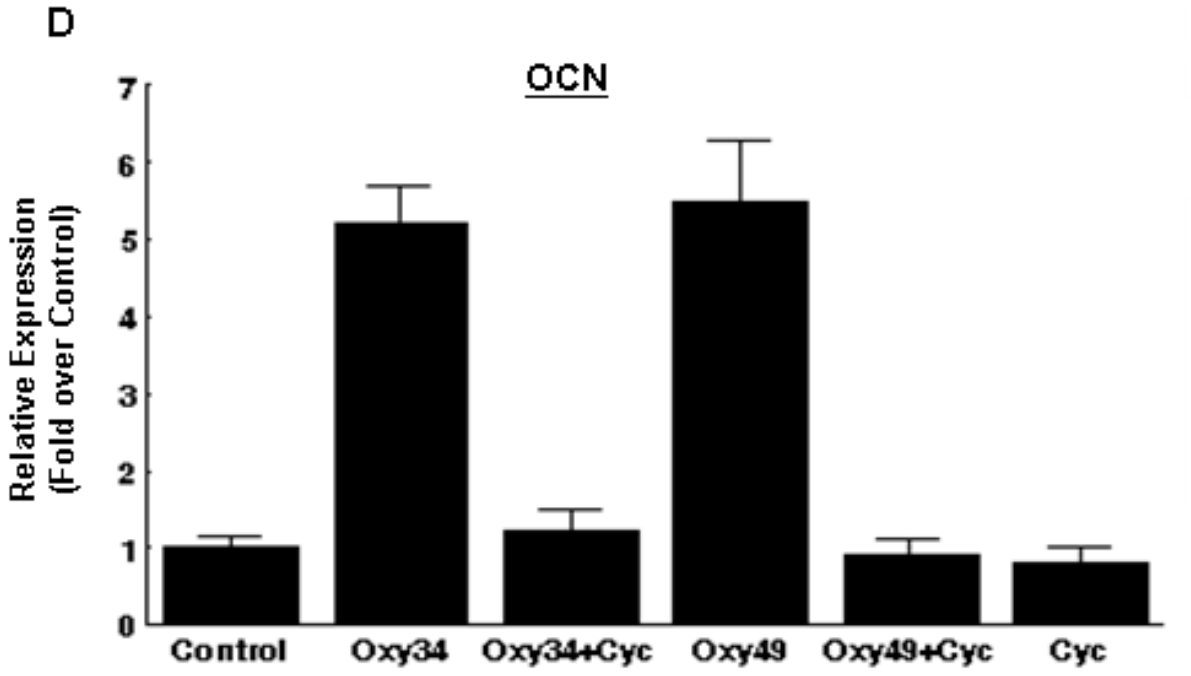

Figure 2D

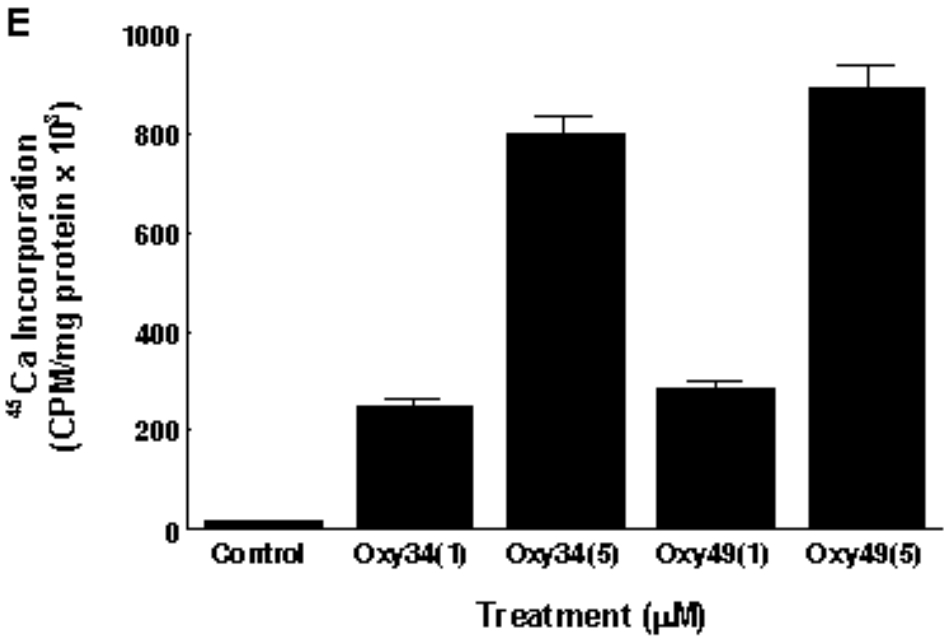

Figure 2E

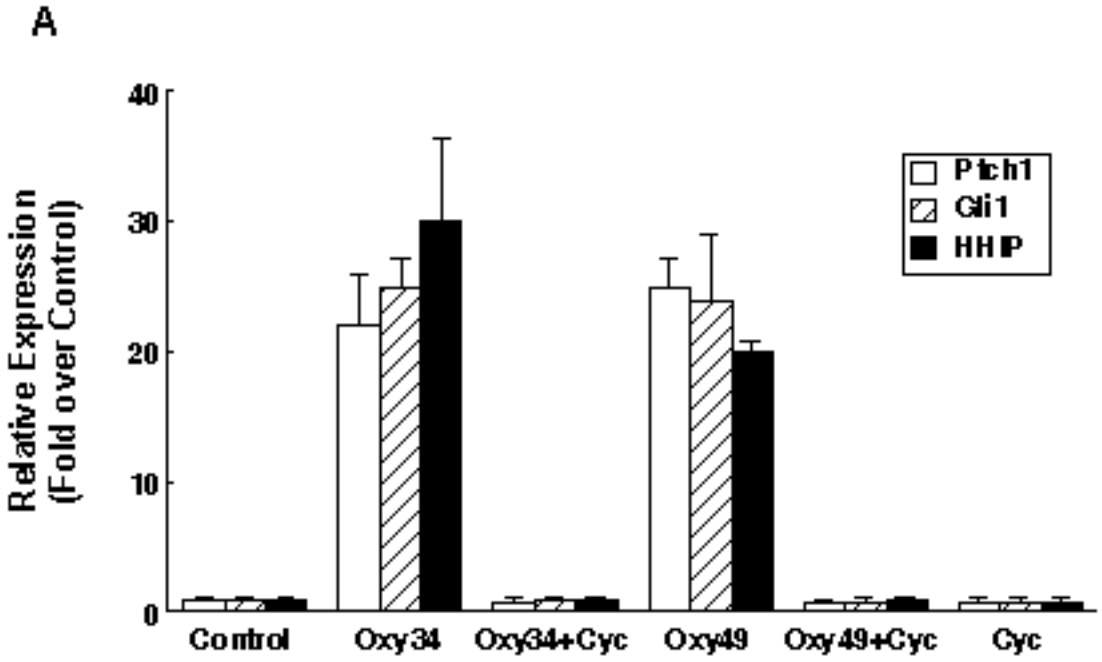

Figure 3A

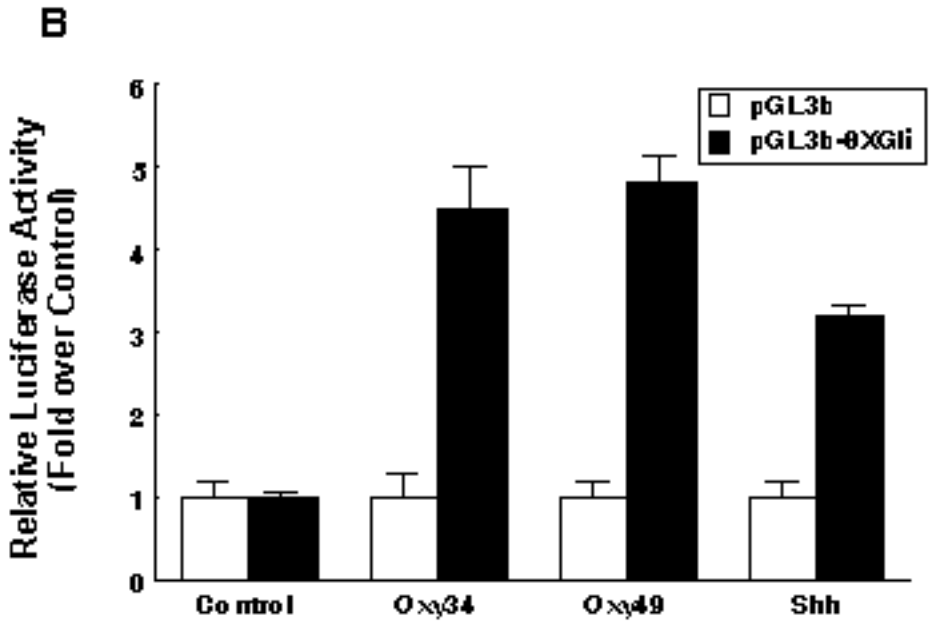

Figure 3B

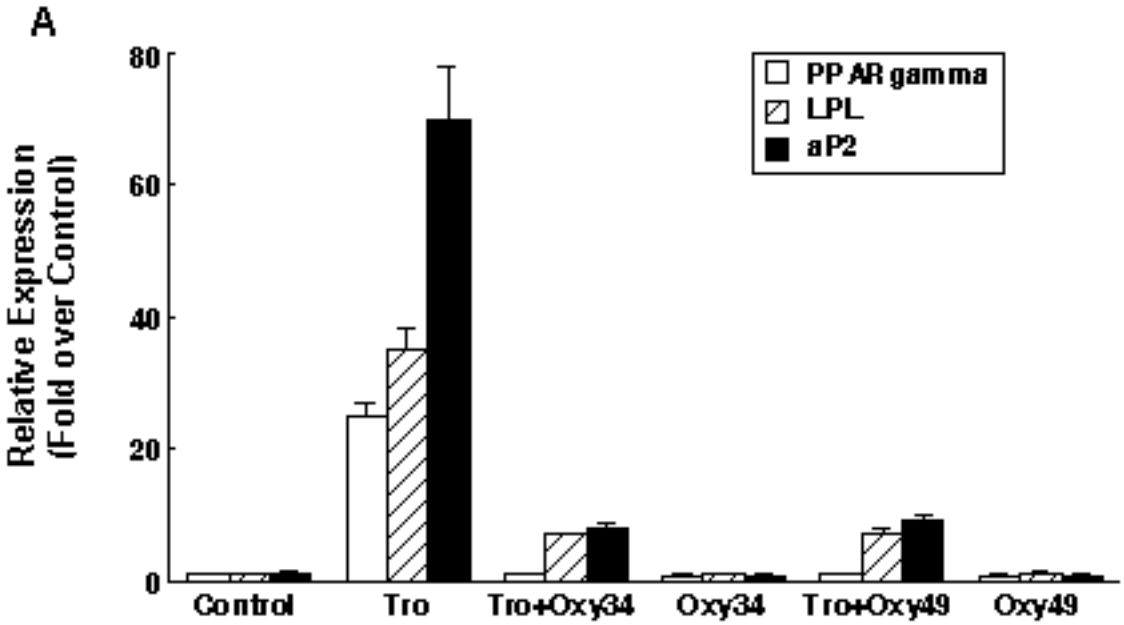

Figure 4A

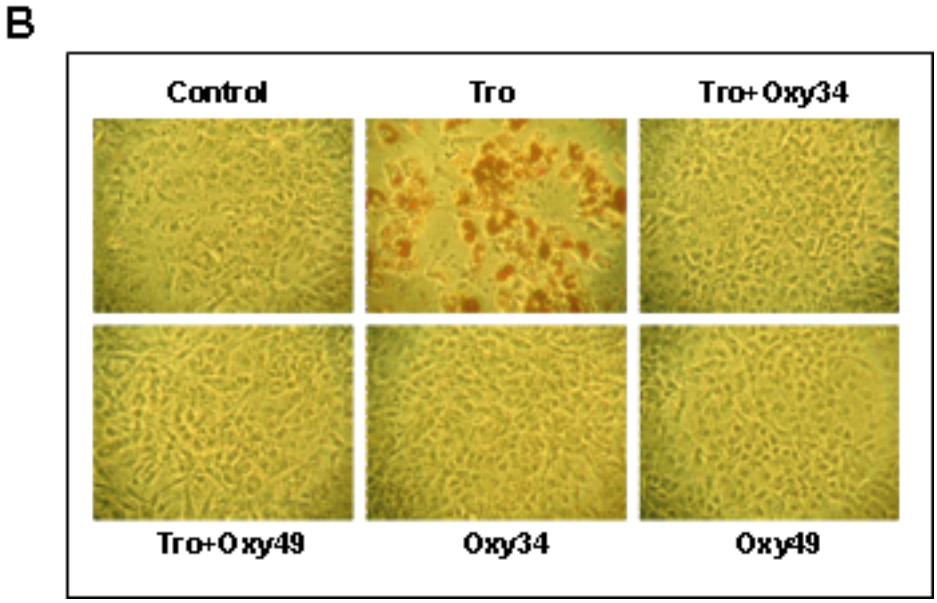

Figure 4B

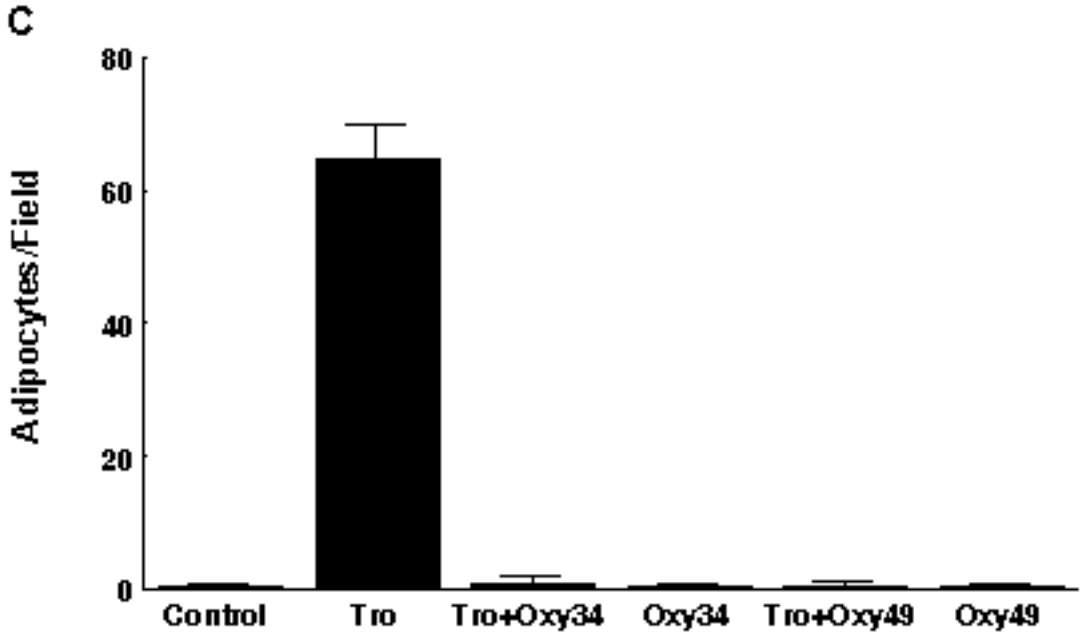

Figure 4C

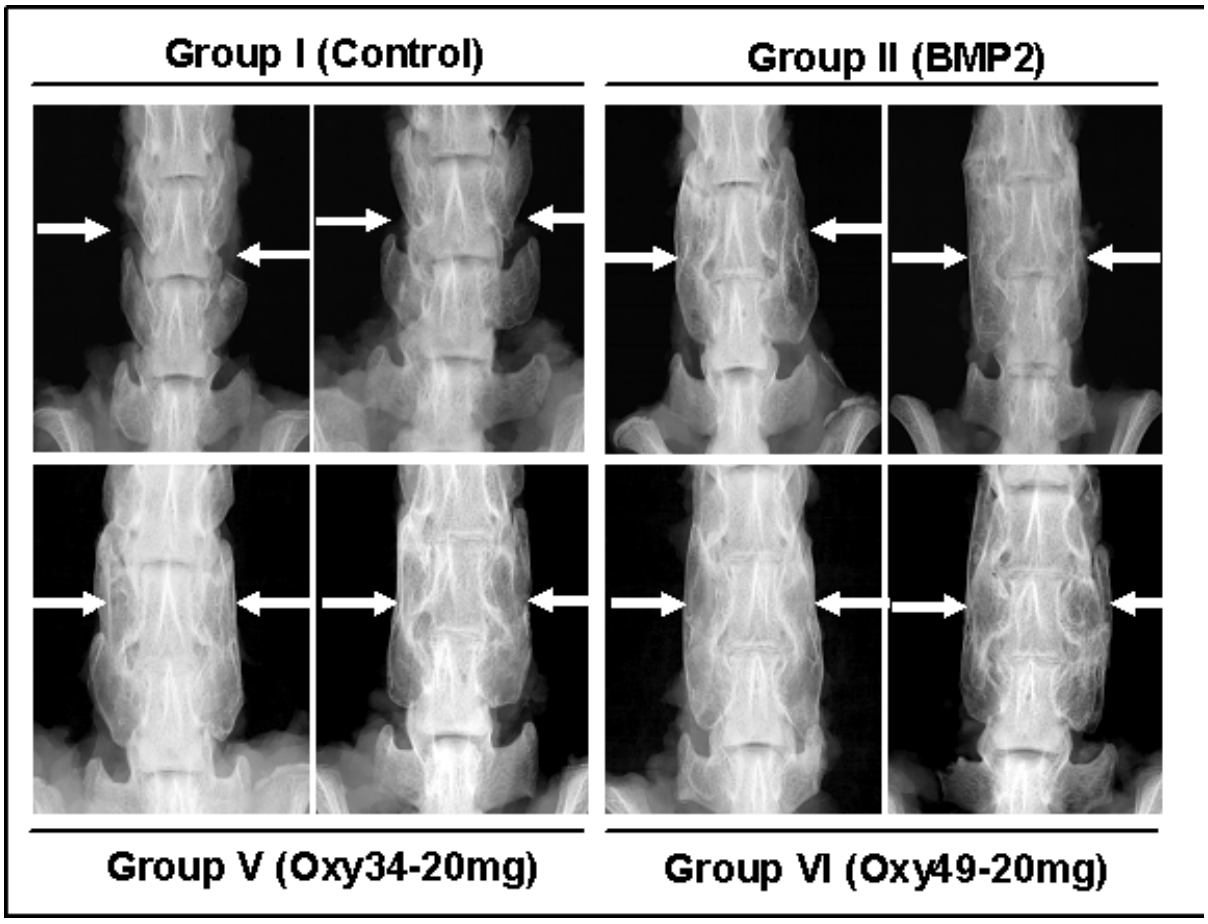

Figure 5

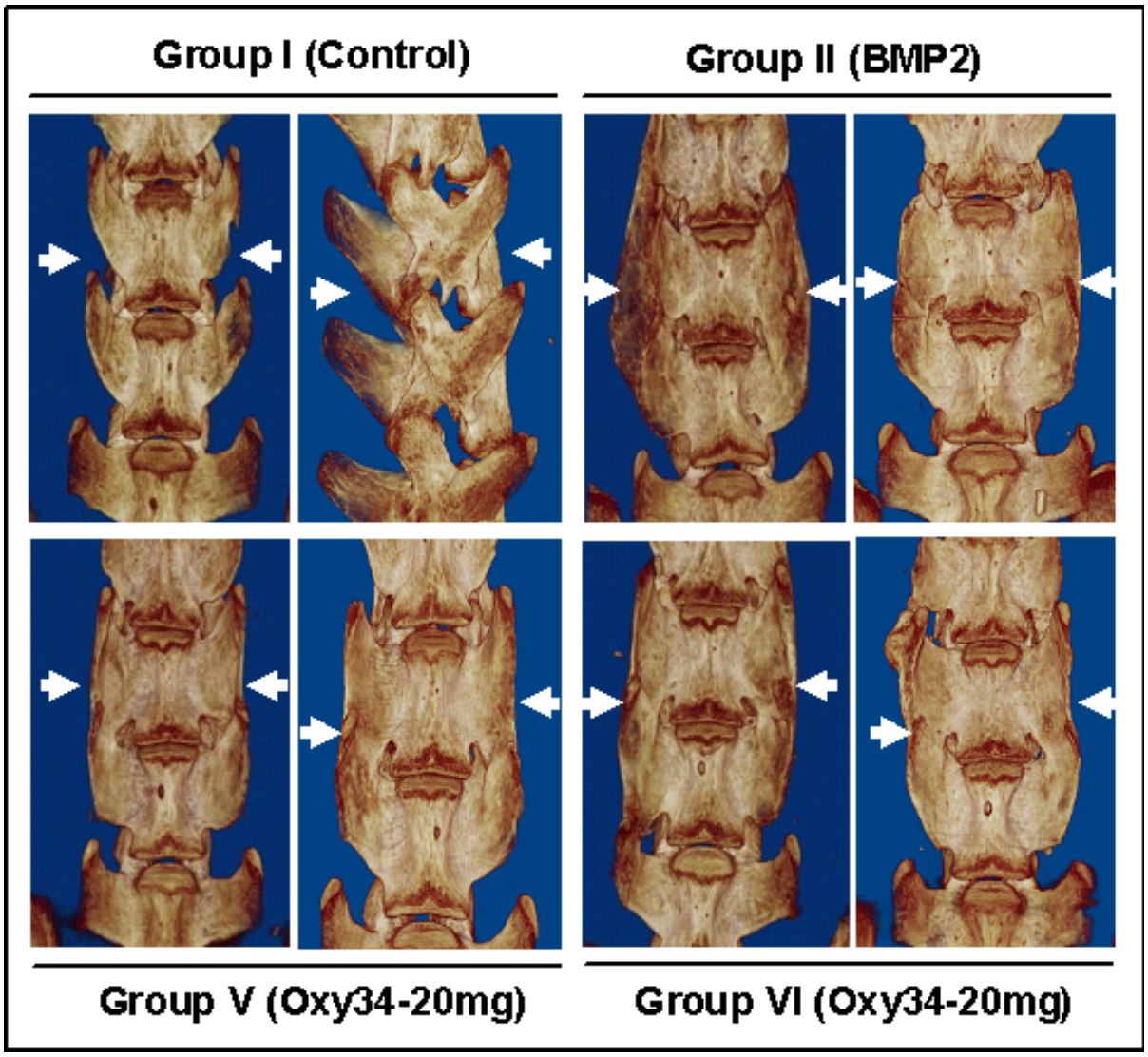

Figure 6

A

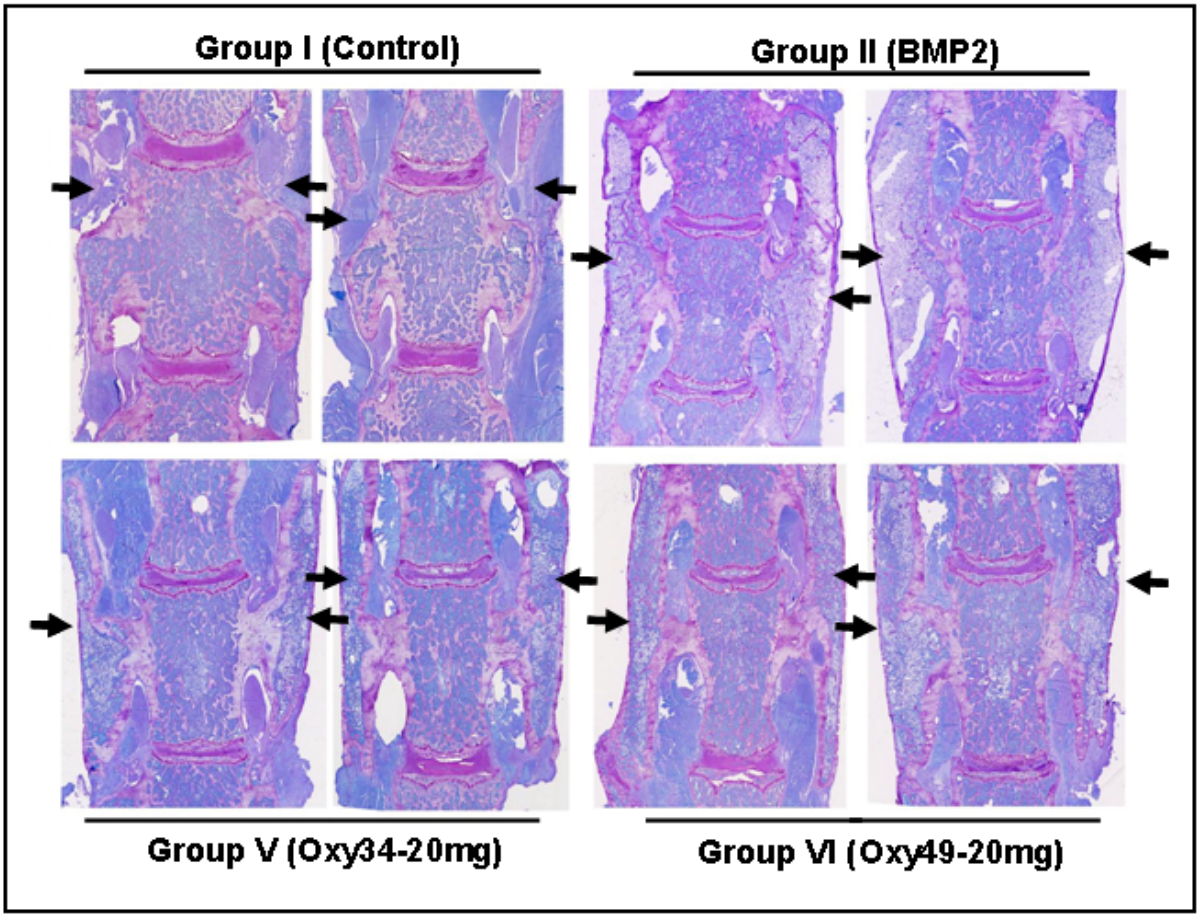

Figure 7A

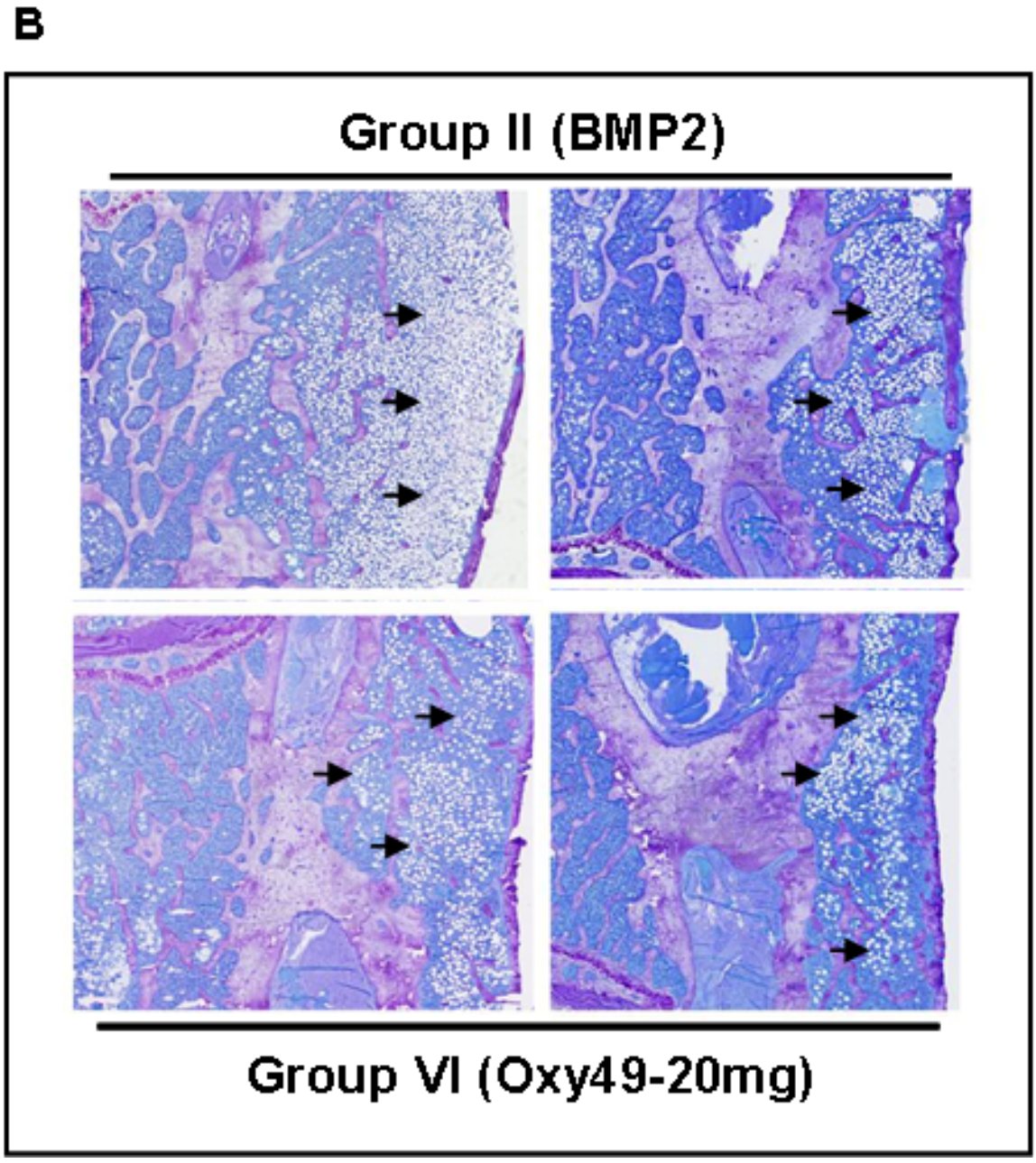

Figure 7B